Journal of Archaeological Science: Reports 56 (2024) 104552

Contents lists available at ScienceDirect

Journal of Archaeological Science: Reports

journal homepage: www.elsevier.com/locate/jasrep

Characterizing ceramic production at Sardis: New insights from neutron activation analysis

Stephen Czujko [a,b,*], Virginie Renson [b], Michael D. Glascock [b,d], Hector Neff [c], Marcus Rautman [a]

[a] Classics, Archaeology, and Religion Department, University of Missouri, Columbia, MO, USA
[b] Archaeometry Laboratory, Research Reactor Center, University of Missouri, Columbia, MO, USA
[c] Anthropology Department, California State University, Long Beach, CA, USA
[d] Anthropology Department, University of Missouri, Columbia, MO, USA

ARTICLE INFO

Keywords:
Ceramics
NAA
Provenance
Sardis
Anatolia

ABSTRACT

This paper presents the results of elemental analysis by neutron activation on 204 ceramics, 11 soils and two modern brick wasters from the site of ancient Sardis in the Republic of Türkiye. Study of these materials is part of collaboration between the Archaeological Exploration of Sardis and the Archaeometry Laboratory at the University of Missouri Research Reactor (MURR). The broader objective of this research is to advance our understanding of the changing nature of Sardis' interactions within the wider region of western Anatolia, from the Archaic to the Late Roman periods. Using the concentrations of 33 elements, we identify and characterize the composition of the ceramics to establish a baseline for future provenance research at the site. Sixteen compositional groups have been identified and separated local production from potential imports. Two robust and well-defined groups characterize most of the local production at the site. Eleven groups are likely composed of imports and three other groups are composed of ceramics that could be local or imported. Thirty-one samples are unassigned. The preliminary results presented here lay the foundation for broader comparison with other databases for ceramics from Sardis and western Anatolia.

1. Introduction

Sardis is located near the village of Sart in the Manisa province of western Türkiye. Situated in the Hermus River plain below the Bozdağ mountain range, the site lies along longstanding paths of communication linking the Aegean coast and Anatolian interior (Fig. 1). Sardis rose to historical prominence in the Early Iron Age as the capital of the Lydian empire (7th–6th centuries BCE), and later served as the base of Achaemenid power in western Asia (6th–4th centuries BCE). Between the 1st century BCE and 7th century CE, it was a major Roman city and Late Roman provincial capital (Hanfmann and Waldbaum, 1975; Cahill, 2010).

The historical development and regional importance of Sardis appear clearly in the ceramic record of the site. The expansion of political power in the mid-1st millennium BCE brought long-lived Anatolian traditions into closer contact with cities along the Aegean coast (Greenewalt, 2010). Later changes in making and using pottery at Sardis reflect new relations within wider networks of exchange. Analysis of fine, utilitarian, and architectural ceramics offers an important perspective of local settlement in antiquity, with bulk elemental analysis contributing to our understanding in new ways.

During the past two decades, bulk elemental analysis has been conducted by neutron activation (NAA) at MURR on material collected by the Archaeological Exploration of Sardis in view to gain a better understanding of the production and circulation of ceramics at Sardis. The purpose of the present paper is to make available a new NAA dataset that includes Roman wares, which have not been the subject of previous analysis, and in so doing lay the foundation for more discursive, archaeologically-based discussion. This paper presents the results of the elemental analysis obtained by NAA of 204 ceramics from the site dating from the Archaic to Late Roman periods. Eleven soil samples and two modern brick wasters were collected in the general vicinity of the site. The groups identified here hold important clues for understanding the range of local signatures and suggest consumption patterns of imported ceramics across time.

Our results constitute a reference for future comparison with existing NAA compositional data from Sardis and western Anatolia produced by other laboratories (Hughes, 1988; Akurgal et al., 2002; Kerschner, 2005;

* Corresponding author at: Archaeometry Laboratory, Research Reactor Center, University of Missouri, Columbia, MO, USA.
E-mail address: scc7w@mail.missouri.edu (S. Czujko).

https://doi.org/10.1016/j.jasrep.2024.104552
Received 8 November 2023; Received in revised form 12 April 2024; Accepted 19 April 2024
Available online 11 May 2024

Fig. 1. Map of western Anatolia with Sardis and related sites.

Kerschner and Mommsen, 2009; Kealhofer et al., 2013; Gürtekin-Demir et al., 2022). Different chemical methods have been used to study archaeological ceramics from Sardis and its surrounding regions (Dupont and Lungu, 2020). The extent to which these results agree can broadly be assessed. Our results expand understanding of the changing nature of Sardis' interactions within western Anatolia.

2. Materials and methods

The 204 ceramics analyzed represent 29 different typologies and a range of shapes. Details of date, function, and type of each sample are provided in Appendix 1. Ceramics come from across the ancient city site being studied by the Archaeological Exploration of Sardis and date between the Archaic and Late Roman periods (i.e., the 7th century BCE to the 7th century CE). The selection of samples was weighted inversely to their previous study, which has focused on the Early Iron Age. Early materials include the well-known Lydian and Late Lydian wares that were common at the site in the Archaic period. Recognized examples include black-on-red stemmed dishes, wave-line hydrias/kraters, oinochoai, skyphoi with banded or streaky glaze decoration, and architectural terracottas (n = 39; for extensive discussion and illustration, see Greenewalt, 1978,2010; Ramage et al., 2021,1-18). Hellenistic and early Roman samples include red- and gray-fired moldmade relief bowls, red-gloss sigillate dishes, and reduction-fired tableware of presumed local manufacture (n = 38; see Rotroff and Oliver, 2003; Rotroff, 2018). Less well-known examples of Late Roman ceramics include red- and black-slipped tableware, plain utility vessels, specialized transport jars, Asia Minor-type lamps, bricks, and rooftiles (n = 125; see Rautman, 1995). Two tiles made by a local factory were included for comparison. The 11 soil samples come from the Sardis vicinity, and like local ceramics are generally of fine texture with small particles of quartz, untwinned feldspar and chert (Gürtekin-Demir 2021, 1-8; Ramage et al., 2021, 9).

The chemical characterization of the ceramics and soils from Sardis was done at MURR using a standard set of procedures that have been described in other publications (Glascock, 1992,2019). For the ceramics, a portion of about 1 cm^2 was sampled for each sherd. The surface of the sample was abraded with a silicon carbide tool to remove any trace of paint, glaze, and other contaminants. The sample was then rinsed and dried under a heat lamp. The soil samples were heated up to 650°C for four hours. Both the ceramic and soil samples were powdered with an agate mortar and pestle. All powders were dried in an oven for a minimum of 24 h at 105°C. An aliquot of 100 mg was used for short irradiations and a second aliquot of 200 mg for long irradiations. Standard reference materials SRM-1633a Coal Fly Ash and SRM-688 Basalt Rock from the National Institute of Standards and Technology (NIST) were similarly prepared, along with an in-house standard Ohio Red Clay used as a quality control. Two irradiations and three measurements were used to determine the concentrations of 33 elements. The irradiation and

Table 1
Experimental parameters and elements measured by NAA at MURR.

Irradiation & count number	Neutron flux ($n \cdot cm^{-2} \cdot s^{-1}$)	Irradiation, decay & measurement times	Elements measured in each count
1-short	8 x 10^{13}	5 sec; 25 min; 12 min	Na, Al, K, Ca, Ti, V, Mn, Ba, Dy
2-medium	6 x 10^{13}	24 hr; 7–8 day; 30 min	As, La, Nd, Sm, Yb, Lu, U
3-long		24 hr; 21–27 day; 3 hr	Sc, Cr, Fe, Co, Ni, Zn, Rb, Sr, Zr, Sb, Cs, Ce, Eu, Tb, Hf, Ta, Th

measurement details are listed in Table 1. The concentrations for all measured elements, along with relevant descriptive information, are listed in Appendix 1. Typical measurement uncertainties range from 2 % to 5 % for most elements, except for As, Ba, Ca, Nd, Sr, and Zr, which range from 5 % to 10 %, and Ti and Zr, which range from 10 % to 20 % (Glascock, 1992).

3. Results

Details on compositional data treatment of archaeological materials are presented elsewhere (e.g., Baxter and Buck, 2000; Bieber et al., 1976; Bishop and Neff, 1989; Glascock, 1992,2019; Harbottle, 1976; Neff, 2000,2002). Here, a principal component analysis (PCA) was performed on the base-10 logarithm transformed dataset, using all 33 elements measured by NAA. Note: all statistical procedures were done using an internally developed GAUSS software program for our lab, MURRAP (https://archaeometry.missouri.edu/gauss.html). The use of log concentrations rather than raw data is advantageous because it compensates for differences in magnitude between the major elements, such as aluminum, and trace elements, such as the rare earth or lanthanide elements (REEs). Transformation to base-10 logarithms also yields a more normal distribution for many trace elements.

Scatterplots of the principal components displaying the distributions of individual samples are shown in Figs. 2 and 3. Fig. 2 shows PC1 versus PC2 which accounts for 57.6 % of the overall variance, and Fig. 3 shows PC1 versus PC3 which accounts for 51.9 % of the variance. During the investigation, both local and non-local wares were identified. Group assignments were initially based on trends seen across hierarchical cluster analysis and scatterplots of different PC pairs.

Table 2 lists the variance (%) and cumulative variance (%) for each of the 33 PCs. The first nine PCs accounted for > 90 % of the variance. See Table 3 for a summary of the scoring coefficients for the first four PCs. The scoring coefficients for each element are representative of that variable's contribution to each PC listed. For PC1 which accounts for 41.6 % of the overall variance, the elements As (0.25), Sb (0.45), and Cs (0.24) contribute positively; whereas Ca (−0.43), Cr (−0.13), and Ni (−0.18) contribute negatively. The elements driving PC2, which explains 16.0 % of the variance, are Hf (0.16), Zr (0.13), Ca (−0.39), and Cr (−0.24). For PC3, the elements Na (0.26) and Ni (0.30) contribute positively, while Cs (−0.52) contributes negatively.

The results show the presence of ten primary compositional groups. Compositional groups can be viewed as "centers of mass" in the compositional hyperspace. Groups are characterized by the locations of their centroids and the unique relationships (i.e., correlations) between the elements. The list of samples, time period, and typologies forming each compositional group is provided in Table 4 and summarized below. Note: the groups are named A-K, but the letter 'I' was skipped to minimize confusion.

Samples are distributed among ten primary compositional groups. The first nine (identified by letters A-J) are surrounded by confidence ellipses that are projected at the 90 % interval (Figs. 2 and 3). This does not mean that the ellipses contain 90 % of the observations. Confidence ellipses have to do with the unobserved population. The variance of the underlying population relates to the confidence ellipse. A high variance will show that the data are diffuse, and consequently the confidence ellipse will be larger than if the variance were smaller. This has implications for interpreting the figures below. As a note, Group K is too small to calculate an ellipse. The soil samples and the unassigned pottery (UNAS) are plotted in the figures as well. Fig. 3, for PC1 versus PC3, offers an alternative viewing of these groups.

Compositional group A (n = 91) includes a range of Archaic, Hellenistic, Roman, and Late Roman wares and styles that are common to Sardis. Two soil samples, SRD145A and 145B, collected near Sardis at Mersindere (5 km west of Sardis), have a signature compatible with group A. Group B (n = 10) is composed of Archaic, Hellenistic, and Late Roman ceramics that are similarly common to Sardis. Roman-period ceramics are absent from this smaller group and no soils or wasters match it. Refer to Table 4 for a more detailed breakdown of these two groups.

Group C (n = 6) belongs to the Roman period and is defined by examples of a red-gloss ware with observed ties to Eastern Sigillata B (ESB), which was made in the Great Meander Valley in western Anatolia. No soil signatures match it. Group D (n = 6) is a collection of Late Roman types and forms that includes two examples of so-called Asia Minor Light

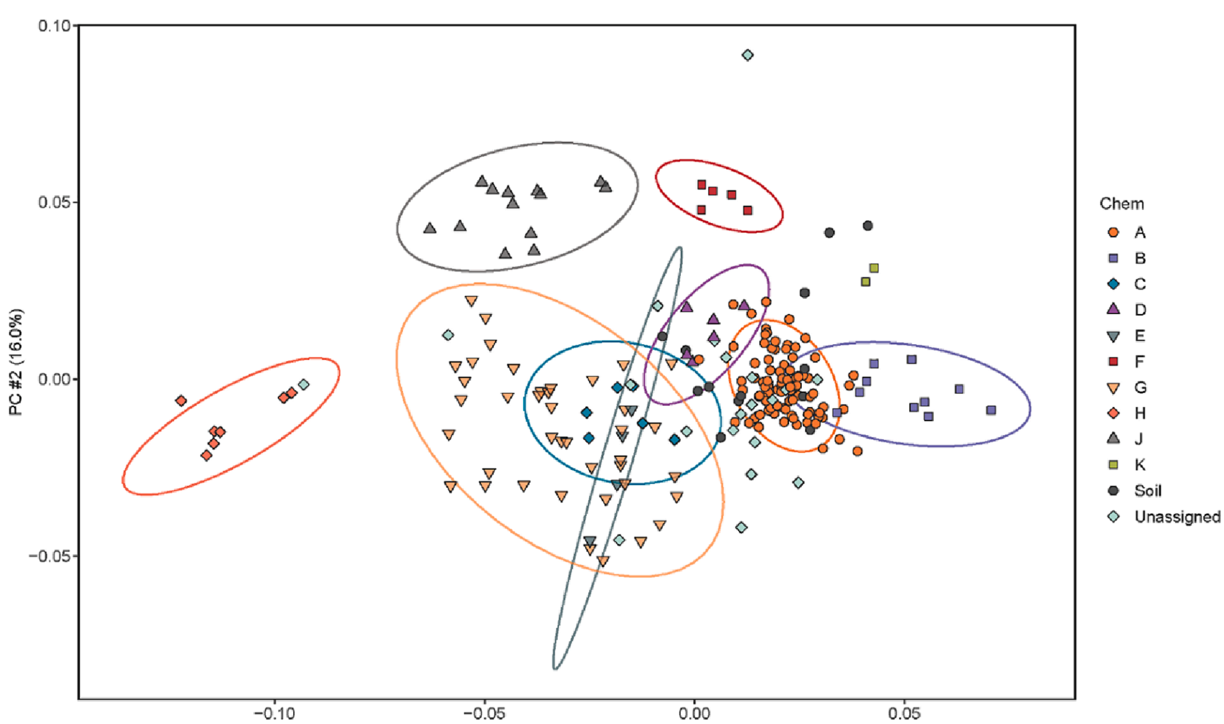

Fig. 2. Scatterplot of Principal Component 1 versus Principal Component 2.

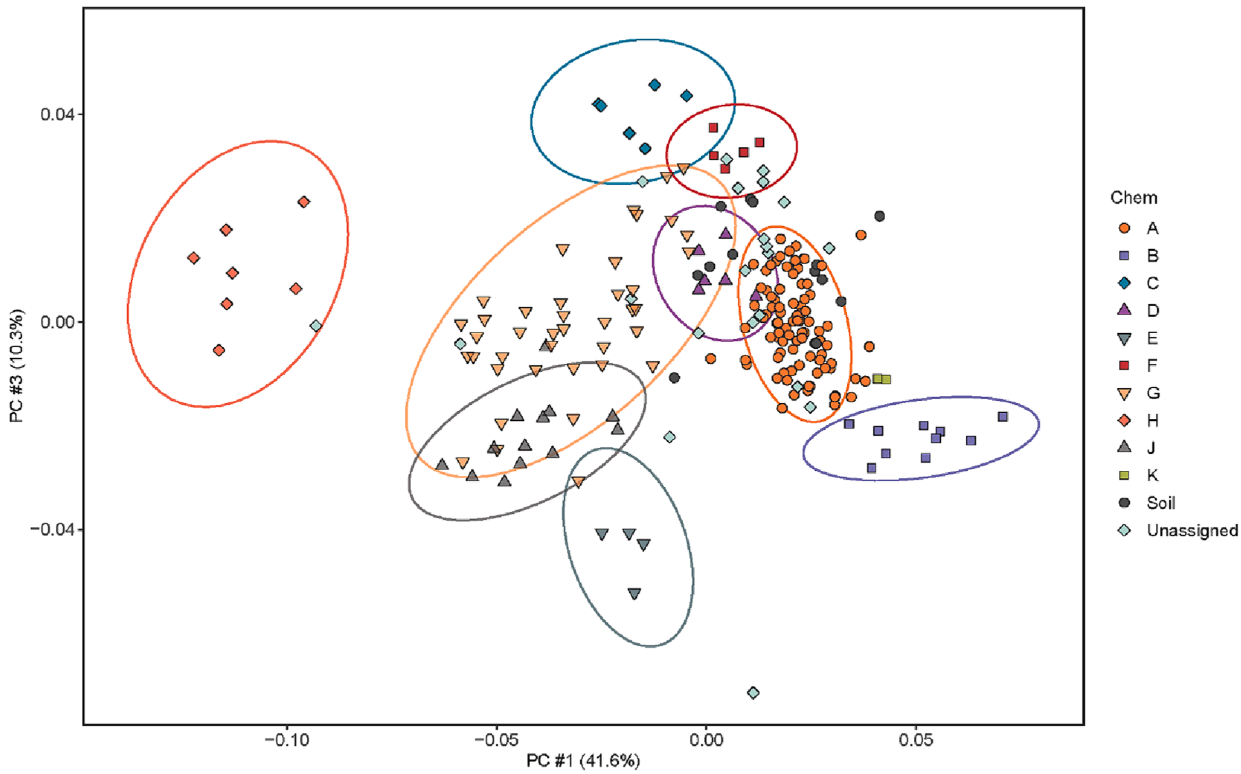

Fig. 3. Scatterplot of Principal Component 1 versus Principal Component 3.

Table 2
Variation (%) and cumulative variation (%) for principal components.

PC	% var.	% cum.	PC	% var.	% cum.
1	41.6	41.6	**18**	0.3	98.4
2	16.0	57.6	**19**	0.3	98.7
3	10.3	67.9	**20**	0.3	99.0
4	6.1	74.0	**21**	0.2	99.2
5	5.5	79.5	**22**	0.2	99.4
6	4.0	83.5	**23**	0.1	99.5
7	3.1	86.6	**24**	0.1	99.6
8	2.7	89.4	**25**	0.09	99.70
9	1.9	91.2	**26**	0.07	99.77
10	1.6	92.8	**27**	0.06	99.83
11	1.3	94.1	**28**	0.05	99.88
12	1.0	95.0	**29**	0.04	99.93
13	0.9	95.9	**30**	0.04	99.96
14	0.8	96.7	**31**	0.02	99.98
15	0.6	97.2	**32**	0.01	100.00
16	0.5	97.7	**33**	0.00	100.00
17	0.4	98.1			

Colored (AMLC) ware, a lamp, one micaceous amphora, and two common (here, micaceous) dishes known broadly as Late Roman C (LRC) ware. The soils SRD143A, 143B, 144A, and 144B, which were obtained about 20 km west of Sardis, show moderate agreement with this group.

Group E (n = 4) includes two examples of Late Roman Çandarlı ware and two of AMLC ware. Group F (n = 5) is represented by gray-fabric micaceous water jar C. No soil signatures match groups E or F. Group G (n = 40) contains samples of mixed typology from the Hellenistic, Roman, and Late Roman periods, most of which have connections to the western Anatolian coast, such as Pergamene Appliqué, Ionian Platters, AMLC ware, and Çandarlı ware. See Table 4 for a full listing of members. No soils match it.

Compositional group H (n = 7) consists of one example of the Roman red-gloss Eastern Sigillata A (ESA) ware and six Late Roman 1 (LR1) amphorae. No soil signatures match group H either. Compositional

Table 3
Scoring coefficients for PCs 1–4 (explaining 74% of variance).

Variable	PC1	PC2	PC3	PC4
Na	0.158	0.027	0.263	−0.074
Al	0.131	0.022	−0.030	0.049
K	0.128	−0.006	−0.033	0.043
Ca	−0.431	−0.391	0.267	−0.298
Sc	0.109	−0.016	0.016	0.121
Ti	0.040	0.060	−0.023	0.034
V	0.136	0.033	0.030	0.114
Cr	−0.133	−0.240	0.094	0.322
Mn	0.063	−0.235	0.121	0.093
Fe	0.151	−0.037	0.054	0.151
Co	0.057	−0.110	0.120	0.278
Ni	−0.180	−0.284	0.301	0.554
Zn	0.114	0.024	0.074	0.140
As	0.246	−0.444	0.228	−0.422
Rb	0.113	0.012	−0.075	0.005
Sr	−0.124	−0.152	0.233	−0.281
Zr	0.060	0.133	0.072	−0.131
Sb	0.453	−0.384	−0.111	0.075
Cs	0.240	−0.376	−0.524	−0.078
Ba	0.221	−0.055	0.101	−0.030
La	0.145	0.071	0.126	0.015
Ce	0.151	0.071	0.136	0.017
Nd	0.155	0.120	0.139	−0.031
Sm	0.175	0.061	0.165	0.022
Eu	0.168	0.033	0.150	0.064
Tb	0.152	0.097	0.346	−0.014
Dy	0.189	0.066	0.176	−0.014
Yb	0.125	0.079	0.120	−0.024
Lu	0.106	0.079	0.099	−0.013
Hf	0.038	0.159	0.049	−0.178
Ta	0.001	0.096	0.078	−0.044
Th	0.097	0.057	0.094	−0.041
U	0.056	0.093	0.096	−0.070

Table 4
Group assignments of Archaic, Hellenistic, Roman, and Late Roman ceramics.

Compositional Group A (n = 91)			
Archaic	Lydian fine wares, tiles	17	SRD051-055, 101–104, 106, 107, 110, 111, 171, 176, 178, 241
Archaic	Late Lydian fine wares, tiles	10	SRD112-118, 120–122
Hellenistic	Sardis moldmade relief	1	SRD001
Hellenistic	Sardis relief red fabric 2	5	SRD011-015
Hellenistic	Sardis gray moldmade relief	4	SRD016-018, 020
Hellenistic	Ionian Platter	5	SRD021-025
Roman	Sardis red-Gloss/ESB	10	SRD047, 048, 127, 130, 151, 152, 161, 162, 165, 166
Roman	Local red-slipped	1	SRD125
Roman	Micaceous red-slipped	1	SRD126
Late Roman	Local red-slipped/LRC	15	SRD026-030, 201–207, 213, 215, 216
Late Roman	Micaceous water jar B	9	SRD057, 061–063, 066–070
Late Roman	Micaceous red-slipped/LRC	2	SRD210, 211
Late Roman	Sardis plain red utility	6	SRD131, 133–137
Late Roman	Local red-slipped	1	SRD218
Late Roman	Micaceous amphora	2	SRD082, 083
Late Roman	Local gray ware	2	SRD123, 124
Compositional Group B (n = 10)			
Archaic	Lydian fine wares	3	SRD105, 109, 177
Hellenistic	Sardis moldmade relief	4	SRD002-005
Late Roman	Moldmade relief	1	SRD156
Late Roman	Local red-slipped/LRC	1	SRD214
Late Roman	Local red-slipped	1	SRD221
Compositional Group C (n = 6)			
Roman	Red-gloss (ESB)	6	SRD046, 049, 050, 128, 153, 163
Compositional Group D (n = 6)			
Late Roman	Micaceous amphora	1	SRD084
Late Roman	Asia Minor lamp	1	SRD164
Late Roman	Micaceous red-slipped/LRC	2	SRD209, 225
Late Roman	Asia Minor Light Colored	2	SRD235, 237
Compositional Group E (n = 4)			
Late Roman	Asia Minor Light Colored	2	SRD129, 227
Late Roman	Çandarlı ware/ESC	2	SRD167, 222
Compositional Group F (n = 5)			
Late Roman	Micaceous water jar C	5	SRD071-075
Compositional Group G (n = 40)			
Archaic	Late Lydian fine ware	1	SRD119
Hellenistic	Pergamene Appliqué	5	SRD006-010
Hellenistic	Ionian Platter	2	SRD138, 139
Roman	Pergamene Sigillata/ESC	1	SRD159
Roman	Red-gloss/ESB	1	SRD160
Late Roman	Asia Minor Light Colored	17	SRD031-037, 080, 081, 228–233, 238, 240
Late Roman	Çandarlı ware/ESC	4	SRD038-040, 076
Late Roman	Micaceous water jar A	3	SRD056, 058, 059
Late Roman	Micaceous water jar B	1	SRD064
Late Roman	Moldmade relief ware	4	SRD154, 155, 157, 158
Late Roman	Micaceous red-slipped/LRC	1	SRD223
Compositional Group H (n = 7)			
Roman	Red-gloss/ESA	1	SRD170
Late Roman	LR1 amphora	6	SRD090-093, 168, 169
Compositional Group J (n = 13)			
Late Roman	Phocaean Red Slip/LRC	10	SRD041-045, 077–079, 224, 226
Late Roman	Late Roman unguentaria	3	SRD085, 086, 088
Compositional Group K (n = 2)			
Archaic	Lydian fine ware	2	SRD172, 173
Unassigned (n = 20)			
Archaic	Lydian fine ware	6	SRD094, 095, 108, 174, 175, 179
Hellenistic	Sardis gray moldmade relief	1	SRD019
Late Roman	Micaceous water jar A	1	SRD060
Late Roman	Micaceous water jar B	1	SRD065
Late Roman	Late Roman unguentaria	3	SRD087, 089, 217
Late Roman	Sardis plain red utility ware	1	SRD132
Late Roman	Micaceous red-slipped/LRC	4	SRD208, 212, 219, 220
Late Roman	Asia Minor Light Colored	3	SRD234, 236, 239
Soils (n = 11)			
Modern	Clay and brick wasters	13	SRD141-148 (and 140B, 143B, 144B, 145B)

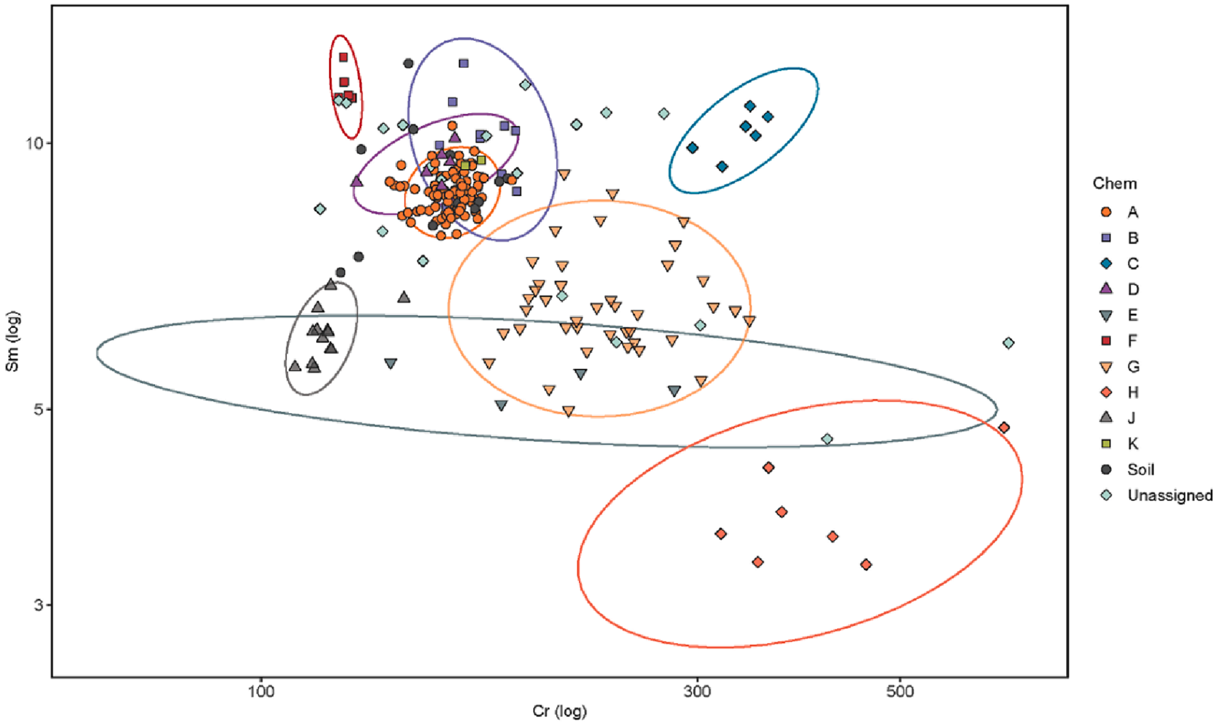

Fig. 4. Log-log scatterplots of Cr versus Sm.

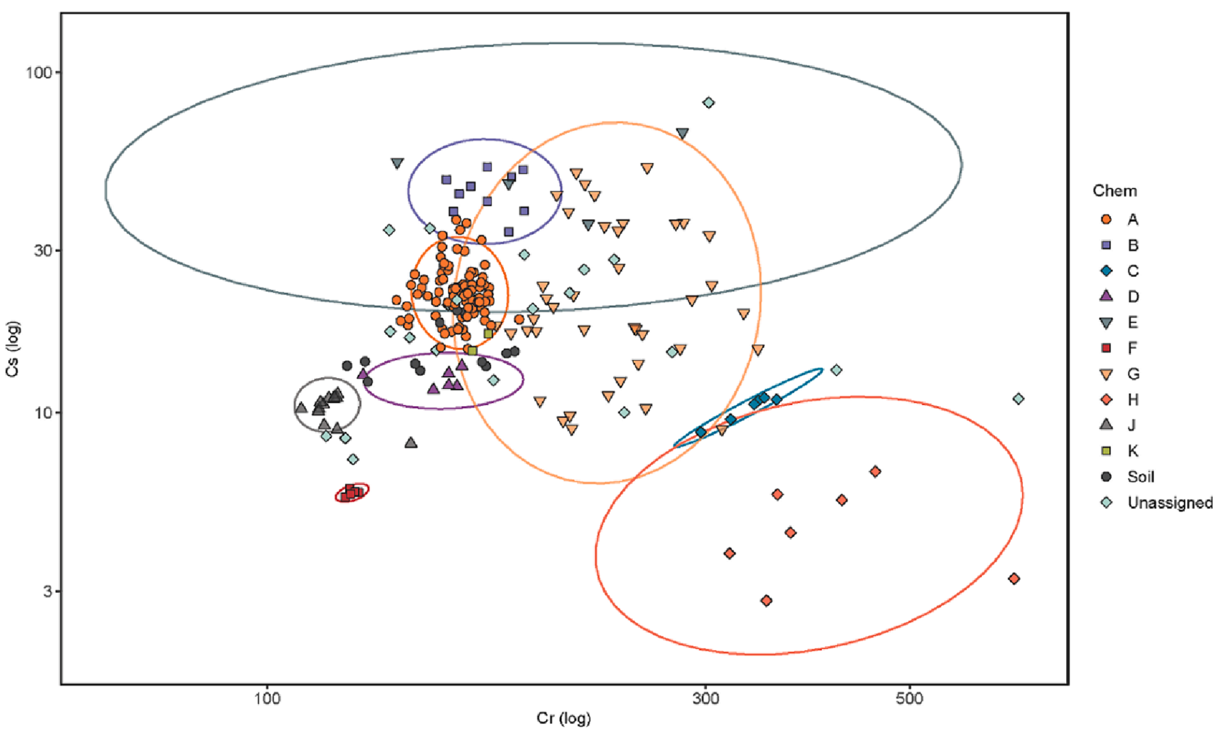

Fig. 5. Log-log scatterplots of Cr versus Cs.

group J (n = 13) is composed of Late Roman wares, with 10 examples of LRC and three Late Roman unguentaria. Two Archaic Lydian examples constitute group K, which are too few to calculate a confidence ellipse. Twenty outliers were left UNAS.

Elemental scatterplots are another method used to examine datasets, evaluate geochemical variability, and identify compositional groups. In this case, plots were reviewed for all element pairs using the base-10 logarithm transformed dataset. The element pairs showing the greatest separation between the groups are included here. Fig. 4 is a scatterplot of Cr versus Sm and Fig. 5 is a scatterplot of Cr versus Cs. Both show the distribution of individual samples and outliers designated as UNAS. Samples are again organized into ten compositional groups.

The group assignments were further evaluated using Mahalanobis distance-based probability calculations. Group members were assigned

Table 5
Subgroup G assignments of Hellenistic, Roman, and Late Roman ceramics.

Compositional Subgroup G-1 (n = 5)			
Hellenistic	Pergamene Appliqué	5	SRD006-010
Compositional Subgroup G-2 (n = 7)			
Late Roman	Asia Minor Light Colored	7	SRD031-033, 035, 080, 233, 238
Compositional Subgroup G-3 (n = 6)			
Late Roman	Asia Minor Light Colored	6	SRD0036, 37, 228, 230, 231, 240
Compositional Subgroup G-4 (n = 3)			
Late Roman	Çandarlı Ware/ESC	3	SRD038, 039, 076
Compositional Subgroup G-5 (n = 3)			
Late Roman	Micaceous water jar B	3	SRD056, 058, 059
Compositional Subgroup G-6 (n = 3)			
Late Roman	Moldmade Relief Ware 3	3	SRD154, 157, 158
Compositional Subgroup G-7 (n = 2)			
Hellenistic	Ionian Platter	2	SRD138, 139
Unassigned (n = 11)			
Archaic	Late Lydian	1	SRD119
Roman	Pergamene Sigillata/ESC	1	SRD159
Roman	Red-Gloss/ESB	1	SRD159
Late Roman	Asia Minor Light Colored	4	SRD034, 081, 229, 232
Late Roman	Micaceous water jar B	1	SRD064
Late Roman	Çandarlı Ware/ESC	1	SRD040
Late Roman	Moldmade Relief	1	SRD155
Late Roman	Micaceous Red-Slipped/ LRC	1	SRD223

using a jackknife procedure to calculate Mahalanobis distance probabilities. Using this procedure, individual samples are removed from their presumed group and treated as if they were "unknowns" before calculating their probability of membership against all groups. Given its large size, all 33 elements were used to evaluate membership assignments to group A. The minimum probability for assignment was 0.001 %. For all other, smaller groups, the first four PCs (explaining 74 % of variance) of the PC-transformed dataset were used and the minimum probability for assignment was a minimum of 1 %. Again, refer to Table 3 for a detailed breakdown of the scoring coefficients for the first four PCs. The probabilities largely confirmed the preliminary groupings but also helped identify the UNAS with probabilities below 1 %. See Table 4 for these group assignments.

3.1. Group G sub-divided

Mahalanobis distance-based probability calculations help confirm the strength of group G. Its constituent members demonstrate a greater likelihood for membership in G than they do to any of the other groups characterized here. However, given the relative size of group G and the large, disperse spread of its members, the group deserves further scrutiny. A separate PCA performed on G suggests that it can be divided into seven subgroups. See Table 5 below for a full breakdown. Fig. 6 is a scatterplot of PC1 versus PC2 that accounts for 56.4 % overall variance, and which displays the plotting of G-1, G-2, G-3, G-4, G-5, G-6, G-7 and 11 not yet assigned to a G subgroup.

The G subgroups are too small to evaluate further using Mahalanobis distance-based probability calculations. Separation between subgroups is observable in the alternative view provided by Fig. 6. Some possible explanations are put forward in the next section. Attempts to divide the other main groups with 10 or more samples – those being A, B, and J – were less productive. They remain coherent and cohesive clusters. Notwithstanding, the total number of compositional groups now equals sixteen.

4. Discussion

Groups A and B are composed of multiple typologies from all time periods represented in this study and probably originated at Sardis. In Fig. 2 for PC1 versus PC2, some initial separation is visible for most of the ten primary groups. Groups A and B overlap with one another. Mahalanobis distance probability calculations suggest that the two soil samples, SRD145A and 145B, exhibit a strong likelihood (greater than 45 %) for assignment to group A. Group A presents a tight clustering and a robust size (n = 91), while group B (n = 10) is a smaller group with samples plotting close to those from group A while remaining clearly distinct. This agrees with the observations of some published XRF and NAA analyses that suggest fairly homogenous, distinct chemical patterns for the site (Kerschner and Mommsen, 2009; Kealhofer et al., 2013; Dupont and Lungu, 2020). Based on the above results, we suggest that groups A and B are representative of ceramic production at Sardis. Further analysis is required to explain the difference in elemental composition between groups A and B. This could indicate the use of different raw materials or preparation recipes at the site.

The origin of some of the other groups depends on comparative analysis. Group C has a composition that differs from local production and includes examples of Eastern Sigillata B, which is believed to originate near Tralles/Aydın, more than 100 km to the south (Takaoğlu, 2006; Civelek, 2010). Consequently, group C is considered as a non-local group. For group D, two of the six samples are AMLC, the origin of which is undetermined but may have come from the region of Çandarlı-Pergamon on the Aegean coast (Hayes 1972, 408-10; Rautman, 1995, 42). The other samples from group D – a micaceous amphora, Asia Minor lamp, and two micaceous red-slipped dishes in the LRC tradition – are associated with broad regional typologies. Of some note are the two LRC examples in group D, which are mica-rich and have fabrics that resemble sediments and clays local to Sardis. This is consistent with some observed local fabric patterns from the Lydian, Late Lydian, and Hellenistic periods (Greenwalt 1978; Dusinberre, 2003; Cahill, 2010; Greenwalt 2010; Dupont and Lungu, 2020). The soils SRD143A, 143B, 144A, and 144B show moderate to strong agreement (20–40 % probability) with group D too, suggesting the possibility that it may indeed belong to the wider environs of Sardis. The picture afforded by this group is a complex one, however. The four samples in group E include AMLC and fine ware made near Çandarlı. Targeted study of the light-colored fabrics that comprise them may help to resolve their origin. The two samples of group K – Lydian fine wares from the Archaic period –are related to one another and appear distinct from the other groups discussed here. Their typology might suggest an origin in Sardis or its wider area. Since the group is small and plots only generally proximate to others, a determination of its origins requires more consideration.

The soils SRD140A, 140B, 147, and 148, as well as the two modern brick wasters SRD141 and 142 were calculated as having comparatively weak probabilities for assignment to any of the groups. At present, the soils' elemental compositions provide limited usefulness. This demonstrates a limitation of elemental data when it comes to relating ceramics to their raw material. Any process that depletes or enriches the clays in specific mineral phases will alter the concentrations of the elements present in these phases (Tite, 2008, 225; Neff et al., 1988,1989; Cogswell et al., 1998). It could also be a function of the limited, non-systematic collection of samples. Earlier attempts to relate local clays and soils to ceramics from Sardis have yielded positive results (Kealhofer et al., 2013).

Groups F, H, and J have signatures that differ from groups A and B and from one another. Figs. 2 and 3 show clear separation of groups F, H, J, and K. The same centers of mass persist across these multiple views, including the elemental biplots of Figs. 4 and 5, often showing a good degree of separation. This serves as an additional check and confirms the strength of group assignments, which are composed of ceramics of likely non-local origin. Group J (n = 13) includes Late Roman unguentaria and LRC wares traditionally associated with Phocaea (Hayes, 1980, lix–lx;

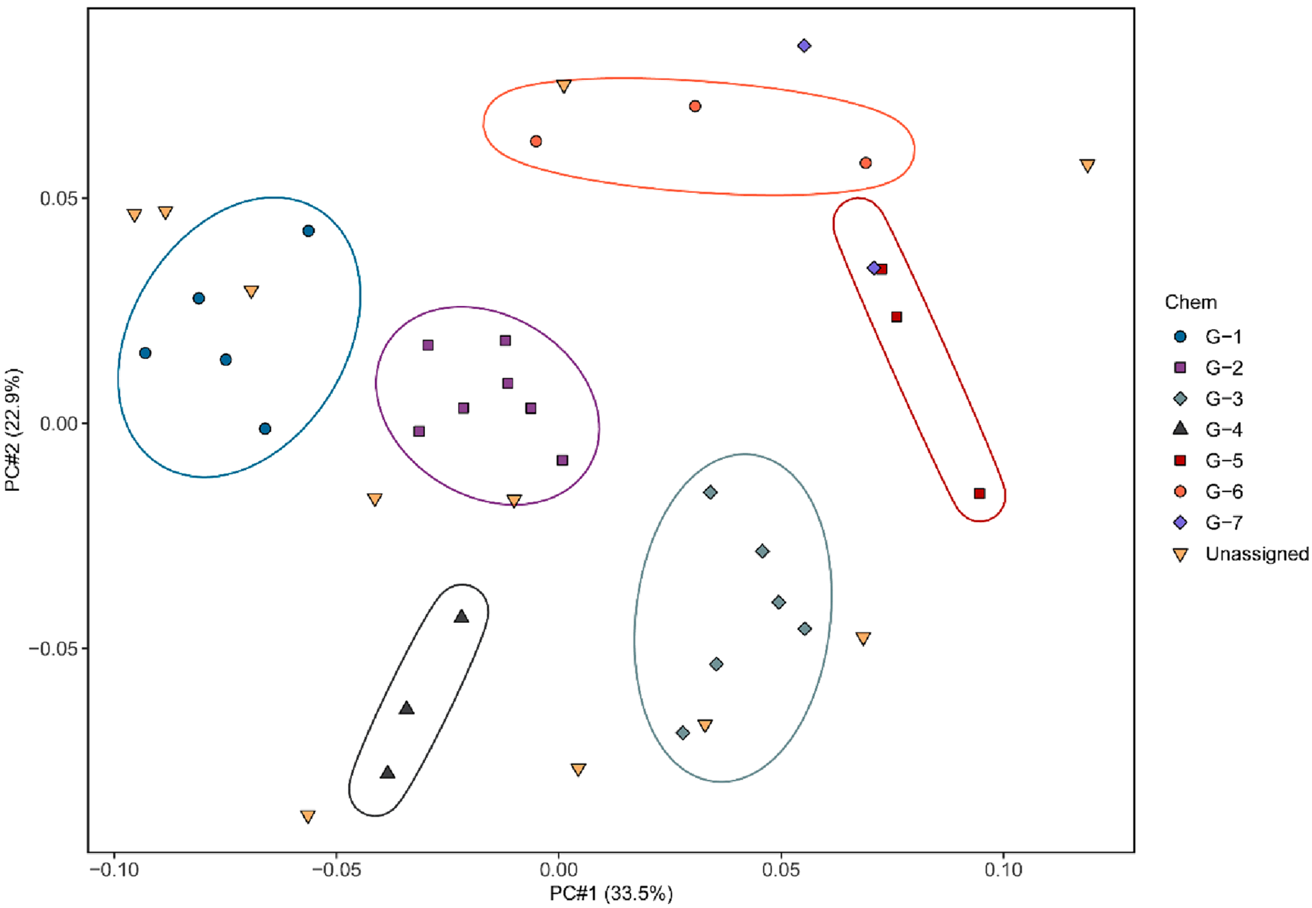

Fig. 6. Scatterplot of Principal Component 1 versus Principal Component 2 in group G PCA.

Vaag, 2005). Recent work from Phocaea, involving land surveys and other archaeometric analysis, has helped to elucidate the scale of this site's productive output (Semiz et al. 2023). Group F (n = 5) is defined by gray-fabric micaceous water jars. The five examples here cluster tightly, but which groups they plot next to change from one figure to the next. Group H, which plots well away from the others, is represented by one example of Eastern Sigillata A ware and six LR1 amphorae, whose origin in Cilicia and north Syria is well established (Slane et al., 1994; Rautman et al., 1999). Comparison with other ceramics of known origin would help confirm these groups' non-local status and their provenance.

Group G is defined by a variety of wares that are clearly imported, like Pergamene Appliqué (n = 5). Others have potentially mixed origins. Group G also contains 17 examples of AMLC wares. See Tables 4 and 5 for a detailed breakdown. Group G does not show the same clear separation in either Figs. 2, 3, and 4 as these last three groups. Instead, group G and its subgroups partially overlap with compositional groups C and E. Group G constitutes a large group whose varied typologies represent wider chemical variability. Closer examination of its subgroups sheds light on the diffuse character of G.

Correlations seem to exist between some of the wares. Subgroup G-1 is solely defined by Pergamene Appliqué (n = 4). Subgroups G-2 (n = 7) and G-3 (n = 6) include only AMLC ware, apparently from two separate sources. Subgroup G-4 (n = 3) is defined by Çandarlı ware, which belongs to the Eastern Sigillata C tradition. G-5 (n = 3) and G-6 (n = 3) are relatively small but internally consistent subgroups. They are composed of two ware types – micaceous water jar A and moldmade relief ware, respectively – that do not have analogs in the other identified main groups. Subgroup G-7 is represented by two Ionian Platters from Mytilene. As the name suggests, this is a ware type that is characterizable by its major finds spots (i.e., along the Ionian Coast, to which Aeolis belongs). Unlike some of the other subgroups, this is one ware type that is also identifiable in group A, which suggests likely production at Sardis. Viewed together these subgroupings reinforce the proposition that they, as well as their parent group, originate near the western Anatolian coast and region of Aeolis. Their overlap is explainable both by the high mobility of products from the leading centers (e.g., Pergamon) and the possibility that more production centers may exist for certain typologies. See Table 6 for a detailed breakdown of the mean elemental compositions for each identified compositional group.

Three main contributions emerge from the analysis presented here. First, our data broadly confirm earlier NAA studies of Archaic Lydian pottery undertaken by other laboratories: the British Museum (Hughes, 1988), the Helmholtz-Institut für Strahlen- und Kernphysik (HISKP) at the University of Bonn (Akurgal et al., 2002; Kerschner, 2005; Kerschner and Mommsen, 2009), and Becquerel Labs in association with the Anatolian Iron Age (AIA) project (Kealhofer et al., 2013). These investigations have characterized the distinctive output of multiple workshops located near Sardis in the Early Iron Age. The HISKP team at Bonn identified two local groups, SarP and SarQ (total n = 59), which are defined by Archaic Lydian-style wares commonly found at the site (Gürtekin-Demir et al., 2022,102-104). The AIA project also identified two local macrogroups A (total n = 206, of which three are sediments) and B (total n = 86, of which 17 are sediments; Kealhofer et al., 2013, table 2a). The Archaic Lydian wares that comprise our groups A and B share stylistic features with these groups and come from the same sources.

Second, our work with Hellenistic and Roman pottery presents an opportunity to extend the study of local ceramic production into later historical eras. Previous analysis has largely focused on materials of the mid-1st millennium BCE. Our data confirm a basic proposition of this

Table 6
Average element concentrations for identified compositional groups.

	A (n = 91)	B (n = 10)	C (n = 6)	D (n = 6)
Element	*M* ± *σ*	*M* ± *σ*	*M* ± *σ*	*M* ± *σ*
Na %	0.980 ± 0.187	0.724 ± 0.143	0.574 ± 0.047	0.719 ± 0.065
Al %	11.4 ± 0.6	12.4 ± 0.6	9.8 ± 0.9	11.0 ± 0.6
K %	3.43 ± 0.24	3.39 ± 0.23	2.94 ± 0.14	3.73 ± 0.38
Ca %	2.33 ± 0.49	1.09 ± 0.55	5.05 ± 1.15	3.29 ± 1.00
Sc	23.8 ± 1.9	24.4 ± 1.1	20.1 ± 1.3	19.2 ± 0.7
Ti %	0.488 ± 0.051	0.475 ± 0.067	0.467 ± 0.045	0.518 ± 0.051
V	173 ± 12	176 ± 11	146 ± 9	150 ± 10
Cr	161 ± 9	174 ± 13	334 ± 22	153 ± 13
Mn	874 ± 83	826 ± 50	895 ± 58	713 ± 38
Fe %	7.08 ± 0.57	7.26 ± 0.54	6.20 ± 0.46	5.64 ± 0.23
Co	27.6 ± 1.5	26.2 ± 1.0	37.8 ± 2.8	25.6 ± 2.2
Ni	74.6 ± 24.5	64.3 ± 13.0	354 ± 41	83.3 ± 11.0
Zn	136 ± 17	119 ± 8	133 ± 15	133 ± 11
As	39 ± 15.2	46.2 ± 17.0	35.3 ± 14.5	27.3 ± 7.3
Rb	162 ± 10	165 ± 7	154 ± 10	170 ± 15
Sr	200 ± 61	136 ± 43	260 ± 86	198 ± 29
Zr	135 ± 26	133 ± 24	121 ± 7	120 ± 21
Sb	5.11 ± 1.21	8.77 ± 1.34	2.46 ± 0.19	3.16 ± 0.55
Cs	23.2 ± 4.6	44.6 ± 6.1	10.3 ± 0.9	12.6 ± 0.8
Ba	724 ± 77	726 ± 78	534 ± 76	707 ± 112
La	46.3 ± 2.2	53.6 ± 5.0	54.7 ± 2.8	52.1 ± 3.0
Ce	94.9 ± 4.5	108.9 ± 10.9	114.0 ± 7.8	106.6 ± 6.0
Nd	41.4 ± 4.6	46.7 ± 4.0	48.3 ± 2.7	46.0 ± 5.0
Sm	8.81 ± 0.5	10.1 ± 1.1	10.3 ± 0.6	9.43 ± 0.45
Eu	1.82 ± 0.08	2.12 ± 0.24	1.97 ± 0.12	1.82 ± 0.11
Tb	1.26 ± 0.34	1.20 ± 0.18	1.54 ± 0.22	1.23 ± 0.14
Dy	6.37 ± 0.55	6.91 ± 0.69	7.59 ± 0.78	6.74 ± 0.82
Yb	3.6 ± 0.26	3.69 ± 0.37	3.75 ± 0.16	3.51 ± 0.06
Lu	0.496 ± 0.033	0.471 ± 0.040	0.494 ± 0.034	0.476 ± 0.024
Hf	4.91 ± 0.8	4.65 ± 0.68	3.76 ± 0.22	4.50 ± 0.38
Ta	1.05 ± 0.07	0.92 ± 0.09	1.29 ± 0.08	1.17 ± 0.07
Th	14.5 ± 0.8	17.1 ± 2.1	19.3 ± 1.2	17.4 ± 1.0
U	3.18 ± 0.58	3.19 ± 0.52	4.08 ± 0.76	4.10 ± 0.54

	E (n = 4)	F (n = 5)	G-1 (n = 4)	G-2 (n = 6)
Element	*M* ± *σ*	*M* ± *σ*	*M* ± *σ*	*M* ± *σ*
Na %	0.363 ± 0.089	0.4 ± 0.054	0.598 ± 0.064	0.801 ± 0.063
Al %	9.9 ± 2.1	8.77 ± 0.15	9.21 ± 0.508	8.26 ± 0.525
K %	2.79 ± 0.20	2.92 ± 0.107	2.8 ± 0.282	3.11 ± 0.173
Ca %	4.57 ± 3.22	5.4 ± 1.16	8 ± 0.81	7.8 ± 1.37
Sc	16.0 ± 2.8	19.4 ± 1.590	18.9 ± 1.23	18.1 ± 2.02
Ti %	0.459 ± 0.057	0.559 ± 0.029	0.483 ± 0.059	0.458 ± 0.045
V	112 ± 14	109 ± 15.6	129 ± 13.3	108 ± 15.3
Cr	207 ± 61	276 ± 38.7	198 ± 10.0	247 ± 31.1
Mn	778 ± 32	809 ± 66.6	909 ± 48.6	807 ± 111
Fe %	4.28 ± 0.55	5.05 ± 0.095	4.86 ± 0.302	4.32 ± 0.364
Co	19.5 ± 2.2	26.0 ± 2.58	24.4 ± 1.87	24 ± 2.42
Ni	102 ± 32	152 ± 27.9	97.3 ± 11.6	133 ± 42.2
Zn	69 ± 3	102 ± 6.38	111 ± 9.58	96.7 ± 9.35
As	24.5 ± 8.1	16.8 ± 1.88	27.5 ± 5.77	64.9 ± 26.5
Rb	147 ± 20	148 ± 4.76	148 ± 8.95	137 ± 13.0
Sr	221 ± 79	368 ± 61.4	215 ± 23.9	169 ± 31.6
Zr	117 ± 20	132 ± 18.1	142 ± 17.4	120 ± 17.9
Sb	6.31 ± 3.09	1.07 ± 0.185	1.80 ± 0.175	2.49 ± 0.413
Cs	51.1 ± 12.9	16.7 ± 1.16	19.3 ± 2.14	32.3 ± 5.62
Ba	556 ± 73	541 ± 70.3	498 ± 73.1	527 ± 66.2
La	35.1 ± 3.8	35.3 ± 0.949	38.0 ± 1.82	38.7 ± 2.85
Ce	68.0 ± 4.6	71.6 ± 2.71	77.2 ± 3.70	77.9 ± 4.91
Nd	26.4 ± 3.3	32.8 ± 10.1	33.2 ± 2.84	32.8 ± 2.00
Sm	5.37 ± 0.26	6.05 ± 0.166	6.46 ± 0.315	6.92 ± 0.465
Eu	1.13 ± 0.06	1.27 ± 0.059	1.32 ± 0.072	1.34 ± 0.083
Tb	0.65 ± 0.20	0.794 ± 0.098	0.884 ± 0.246	0.913 ± 0.175
Dy	3.56 ± 0.95	4.23 ± 0.145	4.61 ± 0.456	5.50 ± 0.437
Yb	2.06 ± 0.33	2.78 ± 0.267	3.05 ± 0.236	3.06 ± 0.265
Lu	0.340 ± 0.031	0.383 ± 0.006	0.435 ± 0.035	0.427 ± 0.028
Hf	4.06 ± 0.22	4.85 ± 0.266	5.48 ± 0.406	4.82 ± 0.577
Ta	1.11 ± 0.14	1.16 ± 0.067	1.25 ± 0.126	1.14 ± 0.108
Th	13.8 ± 2.7	13.0 ± 0.252	14.2 ± 0.632	16.1 ± 1.25
U	3.72 ± 1.19	2.64 ± 0.228	3.24 ± 0.293	3.31 ± 0.540

Table 6 (*continued*)

	G-3 (n = 4)	G-4 (n = 4)	G-5 (n = 3)	G-6 (n = 3)
Element	*M* ± *σ*	*M* ± *σ*	*M* ± *σ*	*M* ± *σ*
Na %	0.801 ± 0.063	0.53 ± 0.054	0.658 ± 0.103	0.516 ± 0.047
Al %	8.26 ± 0.525	8.39 ± 0.658	9.03 ± 1.08	9.65 ± 0.478
K %	3.11 ± 0.173	2.40 ± 0.152	3.26 ± 0.335	2.15 ± 0.122
Ca %	7.8 ± 1.37	8.39 ± 1.96	6.06 ± 1.54	7.99 ± 1.6
Sc	18.1 ± 2.02	17.7 ± 2.37	19.2 ± 1.26	22.3 ± 1.86
Ti %	0.458 ± 0.045	0.459 ± 0.045	0.406 ± 0.064	0.48 ± 0.024
V	108 ± 15.3	105 ± 18.1	135 ± 7.91	163 ± 20.3
Cr	247 ± 31.1	218 ± 10.7	308 ± 20.4	230 ± 15
Mn	807 ± 111	839 ± 70.4	984 ± 10.6	1003 ± 92.9
Fe %	4.32 ± 0.364	4.73 ± 0.31	5.76 ± 0.399	5.54 ± 0.419
Co	24 ± 2.42	22.8 ± 3.92	33.3 ± 0.84	28.8 ± 1.61
Ni	133 ± 42.2	119 ± 17.0	210 ± 42	113 ± 31.6
Zn	96.7 ± 9.35	84.6 ± 8.95	103 ± 5.74	118 ± 13.1
As	64.9 ± 26.5	28.2 ± 6.62	48.8 ± 21.6	36.7 ± 23.6
Rb	137 ± 13.0	138 ± 6.76	147 ± 10.5	114 ± 9.13
Sr	169 ± 31.6	252 ± 66.0	274 ± 62.9	247 ± 46.6
Zr	120 ± 17.9	107 ± 2.85	117 ± 12.2	166 ± 22.5
Sb	2.49 ± 0.413	1.77 ± 0.468	5.95 ± 0.065	3.42 ± 0.286
Cs	32.3 ± 5.62	44.8 ± 1.93	21.6 ± 2.04	11.2 ± 1.3
Ba	527 ± 66.2	485 ± 27.3	602 ± 138	571 ± 10.9
La	38.7 ± 2.85	32.7 ± 2.89	37.9 ± 4.77	44.7 ± 4.01
Ce	77.9 ± 4.91	63.9 ± 5.00	79.1 ± 9.93	96 ± 9.83
Nd	32.8 ± 2.00	33.9 ± 8.87	27.0 ± 6.17	43 ± 3.01
Sm	6.92 ± 0.465	5.76 ± 0.463	7.21 ± 0.867	8.08 ± 0.756
Eu	1.34 ± 0.083	1.18 ± 0.112	1.43 ± 0.171	1.81 ± 0.165
Tb	0.913 ± 0.175	0.784 ± 0.280	1.57 ± 0.455	1.11 ± 0.127
Dy	5.50 ± 0.437	3.64 ± 0.473	5.60 ± 0.572	6.22 ± 0.229
Yb	3.06 ± 0.265	2.45 ± 0.335	3.07 ± 0.23	3.32 ± 0.429
Lu	0.427 ± 0.028	0.366 ± 0.044	0.447 ± 0.033	0.469 ± 0.06
Hf	4.82 ± 0.577	4.52 ± 0.367	4.24 ± 0.5	6.6 ± 0.572
Ta	1.14 ± 0.108	0.965 ± 0.024	1.07 ± 0.102	1.32 ± 0.087
Th	16.1 ± 1.25	11.8 ± 0.515	15.4 ± 1.76	14.5 ± 1.2
U	3.31 ± 0.540	2.76 ± 0.469	4.12 ± 0.262	2.9 ± 0.85

	G-7 (n = 2)	H (n = 7)	J (n = 13)	K (n = 2)
Element	*M* ± *σ*	*M* ± *σ*	*M* ± *σ*	*M* ± *σ*
Na %	0.555 ± 0.173	0.951 ± 0.242	0.367 ± 0.072	0.852 ± 0.003
Al %	9.45 ± 1.25	5.67 ± 0.93	9.19 ± 0.36	1.23 ± 0.001
K %	2.74 ± 0.122	1.66 ± 0.41	2.66 ± 0.38	3.4 ± 0.2
Ca %	5.72 ± 1.44	13.1 ± 2.9	3.07 ± 1.26	0.718 ± 0.131
Sc	17.3 ± 1.93	15.5 ± 3.6	16.4 ± 1.3	26.1 ± 0.504
Ti %	0.353 ± 0.014	0.35 ± 0.127	0.495 ± 0.024	0.604 ± 0.009
V	123 ± 7.25	104 ± 20	127 ± 14	187 ± 2.65
Cr	212 ± 3.32	418 ± 112	118 ± 8	171 ± 4.79
Mn	921 ± 34.7	764 ± 214	363 ± 56	616 ± 33.0
Fe %	4.97 ± 0.535	3.92 ± 0.9	4.24 ± 0.43	6.91 ± 0.295
Co	22.7 ± 1.54	23.2 ± 5.9	16.3 ± 2.8	30.6 ± 0.622
Ni	118 ± 16.9	172 ± 49	56.6 ± 15	77.1 ± 0.099
Zn	113 ± 20.2	80.8 ± 26.7	108 ± 38	159 ± 3.21
As	60.7 ± 27.7	16 ± 4.9	12.7 ± 4.5	20.0 ± 1.89
Rb	177 ± 4.72	63.7 ± 9.7	158 ± 8	167 ± 3.07
Sr	197 ± 15.5	415 ± 124	182 ± 99	86.6 ± 13.0
Zr	159 ± 34.8	78.4 ± 9.6	152 ± 22	134 ± 4.64
Sb	2.84 ± 0.094	1.01 ± 0.16	1.17 ± 0.13	6.41 ± 0.684
Cs	9.26 ± 0.357	4.64 ± 1.43	10.3 ± 1	16.1 ± 1.33
Ba	799 ± 26.7	333 ± 272	304 ± 41	765 ± 3.2
La	44.2 ± 6.97	20.9 ± 1.7	36.9 ± 2.5	51.3 ± 1.03
Ce	90.6 ± 12.8	41.4 ± 3.7	74.8 ± 4.1	105 ± 2.76
Nd	39.5 ± 4.27	16.8 ± 1	37.3 ± 11.2	57.3 ± 3.2
Sm	8.61 ± 0.899	3.83 ± 0.53	6.08 ± 0.41	11.6 ± 0.5
Eu	1.59 ± 0.267	0.918 ± 0.123	1.13 ± 0.1	2.3 ± 0.06
Tb	1.06 ± 0.157	0.601 ± 0.305	0.89 ± 0.25	2.44 ± 0.28
Dy	7.1 ± 0.012	2.42 ± 0.47	4.41 ± 0.3	8.37 ± 0.27
Yb	3.93 ± 0.341	1.83 ± 0.31	3.09 ± 0.23	3.92 ± 0.21
Lu	0.55 ± 0.084	0.259 ± 0.045	0.438 ± 0.021	0.591 ± 0.01
Hf	5.32 ± 1.08	2.92 ± 0.37	6.32 ± 0.65	5.61 ± 0.05
Ta	1.35 ± 0.031	0.683 ± 0.087	1.38 ± 0.08	1.57 ± 0.03
Th	17.7 ± 0.839	6.85 ± 1.13	15 ± 1	21.4 ± 0.8
U	5.72 ± 0.091	1.95 ± 0.54	3.72 ± 0.36	4.09 ± 0.54

paper by showing the continued activity of Sardis workshops as they adopted new shapes and decorative techniques known from other sources during the mid-1st millennium CE. Our groups F, H, and J highlight this broadening of cultural interaction by showing a range of distinctive non-local ceramic features, whose geographic origins may be clarified by further study.

Finally, our analysis of a broad range of local sediments and ceramic materials from Sardis significantly expands the material and historical context of previous study. Identification of two compositional groups within a large local dataset provides an important opportunity to coordinate results obtained by independent laboratories. Clarifying the relationship of these primary compositional groups will facilitate collaborative work with larger archaeometric datasets assembled across the Mediterranean region.

5. Conclusions

The purpose of the present paper is to make available a new NAA dataset that includes Roman wares, which have not been the subject of previous analysis, and in so doing lay the foundation for more discursive, archaeologically-based discussion. As presented here, the data suggest a continuity of customs of craft and production at Sardis, which itself is a novel insight. They invite new and specific research questions too; what other Late Roman wares were produced at the site? Is it possible to better relate the local sediments with the ceramic materials? How do these data compare to other data reported from the region? To satisfactorily resolve these questions involves a more targeted program of study and the marshalling of certain methods (e.g., isotopic analysis) that fall outside the present scope.

NAA concentrations of 33 elements were generated to identify and characterize the composition of 204 ceramics, 11 soils, and two modern brick wasters from Sardis. Statistical interpretation of the compositional data proposed sixteen compositional groups in the dataset. Two robust and well-defined groups characterize most of the local production at the site. Eleven groups are likely composed of imports and three other groups are composed of ceramics that could be local or imported. The origin of the latter depends on further comparative analysis. A total of 31 samples are unassigned. The preliminary results presented here lay the foundation for broader comparison with other databases for ceramics from Sardis and western Anatolia and open up possibilities for further research.

6. Author statement

This manuscript or a very similar manuscript has not been published, nor is under consideration by any other journal.

CRediT authorship contribution statement

Stephen Czujko: Writing – review & editing, Writing – original draft, Visualization, Validation, Investigation, Formal analysis. **Virginie Renson:** Writing – review & editing, Supervision, Project administration, Funding acquisition, Conceptualization. **Michael D. Glascock:** Writing – review & editing, Supervision, Resources, Methodology, Investigation, Funding acquisition, Formal analysis, Data curation. **Hector Neff:** Writing – review & editing, Methodology, Investigation, Formal analysis. **Marcus Rautman:** Writing – review & editing, Supervision, Resources, Project administration, Methodology, Investigation, Funding acquisition, Conceptualization.

Data availability

Data will be made available on request.

Acknowledgments

All cultural and geological materials from Sardis were exported with permission of the Ministry of Culture and Tourism, Republic of Türkiye, between 1993 and 2015.

Funding

This work was supported in part by National Science Foundation grant #2208558 and earlier NSF grants to the Archaeometry Laboratory at the University of Missouri.

Appendix A. Supplementary data

Supplementary data to this article can be found online at https://doi.org/10.1016/j.jasrep.2024.104552.

References

Akurgal, M., Kerschner, M., Mommsen, H., Niemeier, W.-D., 2002. (with a contribution by Ladstätter, S.), Töpferzentren der Ostägäis, Archäometrische und archäologische Untersuchungen zur mykenischen, geometrischen und archaischen Keramik aus Fundorten in Westkleinasien. Ergänzungsheft Der Jahreshefte Des Österreichischen Archäologischen Institutes vol. 3.

Baxter, M.J., Buck, C.E., 2000. Data handling and statistical analysis. In: Ciliberto, E., Spoto, G. (Eds.), Modern Analytical Methods in Art and Archeology. John Wiley and Sons Inc, Hoboken, pp. 681–746.

Bieber Jr., A.M., Brooks, D.W., Harbottle, G., Sayre, E.V., 1976. Application of multivariate techniques to analytical data on Aegean ceramics. Archaeometry 18, 59–74. https://doi.org/10.1111/j.1475-4754.1976.tb00145.x.

Bishop, R.L., Neff, H., 1989. Compositional data analysis in archaeology. In: Allen, R.O. (Ed.), Archaeological Chemistry IV. American Chemical Society, Washington, D.C., pp. 576–586

Cahill, N.D. (Ed.), 2010. Lidyalılar ve dünyaları / The Lydians and Their World. Yapı Kredi Yayınları, Istanbul. [online: https://sardisexpedition.org/publications/latw/].

Civelek, A., 2010. Red-slip ware from Tralles excavations. Colloquium Anatolicum 9, 169–191.

Cogswell, J.W., Neff, H., Glascock, M.D., 1998. Analysis of shell-tempered pottery replicates: implications for provenance studies. Am. Antiq. 63, 63–72. https://doi.org/10.2307/2694776.

Dupont, P., Lungu, V., 2020. Lydian Sardis and its sphere of influence in the light of laboratory analysis results. Ancient Civilizations from Scythia to Siberia 26, 112–145.

Dusinberre, E.R.M., 2003. Aspects of Empire in Achaemenid Sardis. Cambridge University Press, Cambridge.

Glascock, M.D., 1992. Characterization of archaeological ceramics at MURR by neutron activation analysis and multivariate statistics. In: Neff, H. (Ed.), Chemical Characterization of Ceramic Pastes in Archaeology. Prehistory Press, Madison, pp. 11–26.

Glascock, M.D., 2019. Compositional analysis of archaeological ceramics. In: Glascock, M.D., Neff, H., Vaughn, K. (Eds.), Ceramics of the Indigenous Cultures of South America: Studies of Production and Exchange through Compositional Analysis. University of New Mexico Press, Albuquerque, pp. 1–13.

Greenewalt jr., C.H., 1978. Ritual Dinners in Early Historic Sardis. University of California Press, Berkeley.

Greenewalt, C.H., jr., 2010. Lydian Pottery, in: Cahill, N.D. (Ed.), Lidyalılar ve dünyaları / The Lydians and Their World. Yapı Kredi Yayınları, Istanbul. [online: https://sardisexpedition.org/en/essays/latw-greenewalt-lydian-pottery].

Gürtekin-Demir, R.G., 2021. Lydian Painted Pottery Abroad. The Gordion Excavations, 1950–1973 (Gordion Special Studies 9, University Museum Monograph 156). University of Pennsylvania Museum of Archaeology and Anthropology, Philadelphia.

Gürtekin-Demir, R.G., Mommsen, H., Kerschner, M., 2022. Regional lydian pottery at daskyleion: testing stylistic classification by chemical analysis. Anatol. Stud. 72, 97–116. https://doi.org/10.1017/S0066154622000059.

Hanfmann, G.M.A., Waldbaum, J.C., 1975. A Survey of Sardis and the Major Monuments Outside the City Walls. Harvard University Press, Cambridge, Mass.

Harbottle, G., 1976. Activation analysis in archaeology. Radiochemistry 3, 33–72. https://doi.org/10.1007/3-540-52423-1_3.

Hayes, J.W., 1972. Late Roman Pottery. British School at Rome, London.

Hayes, J.W., 1980. A Supplement to Late Roman Pottery. British School at Rome, London.

Hughes, M.J., 1988. Appendix: The analysis of pottery lamps mainly from western Anatolia, including Ephesus by neutron activation analysis. In: Bailey, d.m., A Catalogue of the Lamps in the British Museum III. Roman Provincial Lamps. British Museum, London, pp. 461–485.

Kealhofer, L., Grave, P., Marsh, B., 2013. Scaling ceramic provenience at Lydian Sardis, Western Turkey. J. Archaeol. Sci. 40, 1918–1934.

Kerschner, M., 2005. Die Ionier und ihr Verhältnis zu den Phrygern und Lydern. Beobachtungen zur archäologischen Evidenz. In: Schwertheim, E. (Ed.), Neue Forschungen Zu Ionien. Bonn, Rudolf Habelt, pp. 113–146.

Kerschner, M., Mommsen, H., 2009. Neue archäologische und archäometrische Forschungen zu den Töpferzentren der Ostägäis. In: Dupont, P., Lungu, V. (Eds.), Les Productions Céramiques Du Pont-Euxin à L'époque Grecque. Actes Du Colloque International, Bucarest, 18–23 Septembre 2004. Edizioni Quasar di Severino Tognon, Rome, pp. 79–93.

Neff, H., 2000. Neutron activation analysis for provenance determination in archaeology. In: Ciliberto, E., Spoto, G. (Eds.), Modern Analytical Methods in Art and Archaeology. John Wiley and Sons Inc, New York, pp. 81–134.

Neff, H., 2002. Quantitative techniques for analyzing ceramic compositional data. In: Glowacki, D.M., Neff, H. (Eds.), Ceramic Source Determination in the Greater Southwest. Cotsen Institute of Archaeology, UCLA, Los Angeles.

Neff, H., Bishop, B., Sayre, E.V., 1988. A stimulation approach to the problem of tempering in compositional studies of archaeological ceramics. J. Archaeol. Sci. 15, 159–172. https://doi.org/10.1016/0305-4403(88)90004-0.

Neff, H., Bishop, B., Sayre, E.V., 1989. More observations on the problem of tempering in compositional studies of archaeological ceramics. J. Archaeol. Sci. 16, 57–69. https://doi.org/10.1016/0305-4403(89)90056-3.

Ramage, A., Ramage, N.H., Gürtekin-Demir, R.G., 2021. Ordinary Lydians at Home: The Lydian Trenches of the House of Bronzes and Pactolus Cliff at Sardis, Sardis R8. Archaeological Exploration of Sardis, Cambridge MA.

Rautman, M., 1995. Two Late Roman wells at Sardis. In: Dever, W.G. (Ed.), Preliminary Excavation Reports: Sardis, Idalion, and Tell El-Handaquq North, AASOR 53. American Schools of Oriental Research, Cambridge, MA, pp. 37–84.

Rautman, M.L., Neff, H., Gomez, G., Vaughan, S., Glascock, M.D., 1999. Amphoras and roof-tiles from Late Roman Cyprus: A compositional study of calcareous ceramics from Kalavasos-Kopetra. Journal of Roman Archeology 12, 377–391. https://doi.org/10.1017/S1047759400018110.

Rotroff, S.I., 2018. Eastern Sigillata at Sardis: Evidence for a local industry. Bull. Am. Sch. Orient. Res. 380, 133–204. https://doi.org/10.5615/bullamerschoorie.380.0133.

Rotroff, S.I., Oliver Jr., A., 2003. The Hellenistic Pottery from Sardis: The Finds through 1994, Sardis M12. Archaeological Exploration of Sardis, Cambridge MA.

Semiz, B., Ok, M., Dumankaya, O., 2024. Archaeometric investigations of the Late Roman period red slip ware from Caesarea Germanicia (Kahramanmaraş, southeastern Anatolia). Archaeometry 1–26. https://doi.org/10.1111/arcm.12946.

Slane, K.W., Elam, J.M., Glascock, M.D., Neff, H., 1994. Compositional analysis of Eastern Sigillata A and related wares from Tel Anafa (Israel). J. Archaeol. Sci. 21 (1), 51–64. https://doi.org/10.1006/jasc.1994.1007.

Takaoğlu, T., 2006. New light on the origins of Eastern Sigillata B ware. In: Takaoğlu, T. (Ed.), Anadolu Arkeolojisine Katkılar 65. Yaşında Abdullah Yaylalı'ya Sunulan Yazılar, Hitit Yayınları, Istanbul, pp. 263–1227.

Tite, M.S., 2008. Ceramic production, provenance and use—A review. Archaeometry 50, 216–231. https://doi.org/10.1111/j.1475-4754.2008.00391.x.

Vaag, L.E., 2005. Phocaean Red Slip ware: Main and secondary productions. In: Briese, M.B., Vaag, L.E. (Eds.), Trade Relations in the Eastern Mediterranean from the Late Hellenistic Period to Late Antiquity: the Ceramic Evidence. University Press of Southern Denmark, Odense, pp. 132–1118.